PROCEEDINGS OF SPIE

SPIEDigitalLibrary.org/conference-proceedings-of-spie

Hyper-Rayleigh scattering measurements of magnetite nanoparticles: determination of the first order hyperpolarizability anisotropy

E. S. Gonçalves, R. D. Fonseca, L. De Boni, A. M. Figueiredo Neto

E. S. Gonçalves, R. D. Fonseca, L. De Boni, A. M. Figueiredo Neto, "Hyper-Rayleigh scattering measurements of magnetite nanoparticles: determination of the first order hyperpolarizability anisotropy," Proc. SPIE 10941, Emerging Liquid Crystal Technologies XIV, 109410G (1 March 2019); doi: 10.1117/12.2510249



Event: SPIE OPTO, 2019, San Francisco, California, United States

Hyper-Rayleigh scattering measurements of magnetite nanoparticles: Determination of the first order hyperpolarizability anisotropy

E. S. Gonçalves^a, R. D. Fonseca^{b, c}, L. De Boni^b, and A. M. Figueiredo Neto^a

^aInstituto de Física, Universidade de São Paulo, São Paulo, SP, Brazil ^bInstituto de Física de São Carlos, Universidade de São Paulo, São Carlos, SP, Brazil ^cUniversidad Popular del Cesar, Barrio Sabana, Campus Universitario, Valledupar, Colombia

ABSTRACT

The hyper-Rayleigh scattering technique was used to determine the first order hyperpolarizability β of magnetic nanoparticles dispersed on colloidal solutions. Pulse trains of mode-locked pulses of 100 ps on an a Q-switcher envelope of 150 ns emitted by a Nd:YAG laser, centered on 1064 nm, were used since this method allows measurements as a function of the incident beam intensity without the need of external elements. In order to determine the procedure to measure second-order optical nonlinearities on magnetic nanoparticles and avoid cumulative effects during the measurements, that lasts between to consecutive pulse trains, the results were studied for different values of the Q-switcher repetition rate, from 5 Hz to 800 Hz. Since cumulative effects were verified for higher values of repetition rates, all measurements were performed at the rate of 30 Hz. Therefore, the first-order hyperpolarizability β was measured in the presence and absence of external magnetic field of magnitude H=800 G. The linear attenuation spectrum was determined and didn't change with the appliance of magnetic field since large aggregates of nanoparticles were not formed. Nonlinear scattering measurements were performed in the case were the laser light polarization was parallel and perpendicular to the external field lines, employing a half-wave plate to change the light polarization state. In the absence of magnetic field, $\beta_{H=0}=8.5(1)\times10^{-28}$ cm⁵/esu, while in their presence of magnetic field, $\beta_{\parallel}=9.8(2)\times10^{-28}$ cm⁵/esu and $\beta_{\parallel}=8.1(1)\times10^{-28}$ cm⁵/esu, showing an anisotropy $\beta_{\parallel}-\beta_{\perp}$ of about 17%.

1. INTRODUCTION

Magnetic colloids or ferrofluids $(FF)^{1-3}$ correspond to nanoparticles with typical dimensions of the order of 10 nm made of magnetic materials, usually magnetite (Fe_3O_4) but recurrently by other ferrites (MFe_2O_4) , in which M is a divalent cation as Co, Mn, Zn or Ni for example), dispersed in a liquid medium. Combining the carrier fluidity and the nanoparticles physical properties, ferrofluids are widely studied and several technological applications¹ rely on their characteristics, from biomedical applications⁴⁻⁷ to optical devices.^{8,9} Optofluidic devices such as magnetic field detectors and magnetometers¹⁰⁻¹² were developed with optical fibers and ferrofluids, as well as optofluidic switchers,¹³ ferrofluid-clad silicon micro-ring resonators¹⁴ allowing the control of resonances by magnetic fields, as well as variable optical attenuators.¹⁵

The most prominent applications of these materials rely on the possibility of changing suspension's physical properties through external magnetic fields. Therefore, the organization dynamics of magnetic nanoparticles was studied $^{16-18}$ through light transmission experiments, 19 as well as magneto-optical properties of ferrofluids 20,21 in the presence of magnetic field, the anisotropy of light transmission 22 and extinction. $^{23-25}$ Despite the existence of several studies on the (linear) interaction between light and ferrofluids, with or without the presence of external magnetic fields, lacks on the literature works on the nonlinear optical 26,27 (NLO) properties of magnetite nanoparticles. Nonlinear refraction and absorption of magnetic nanoparticles were studied as a function of nanoparticles size, 28 on colloidal solutions and thin-films 29 and the modification of these properties due to external

Further author information:

E. S. Gonçalves: e-mail: eduardos@if.usp.br, Telephone: +55 11 3091 6638

Emerging Liquid Crystal Technologies XIV, edited by Liang-Chy Chien, Proc. of SPIE Vol. 10941, 109410G ⋅ © 2019 SPIE ⋅ CCC code: 0277-786X/19/\$18 ⋅ doi: 10.1117/12.2510249

magnetic fields.³⁰ Further studies on this area, in particular second-order nonlinear properties of ferrofluids, besides supporting the development of new optofluidic devices, can also provide understanding of these materials on the fundamental point of view.

Therefore, in this work we seek to determine the procedure to measure second-order nonlinear properties of ferrofluids as well as to provide specific experimental precautions during the measurements that were taken into account in order to evaluate the dependency of these properties with the application of external magnetic fields, recently published.³¹ The measurements and analysis processes were performed using the hyper-Rayleigh scattering (HRS)^{32,33} technique in order to determine the first-order hyperpolarizability β of magnetic nanoparticles dispersed in aqueous solution. The solution was subjected to external magnetic field in order to align the nanoparticles^{3,34} and probe the hyperpolarizability along two directions, parallel and perpendicular to the field.

2. THEORETICAL BACKGROUND

2.1 Magnetic properties of ferrofluids

Each nanoparticle, due to it's reduced size, presents only one magnetic domain, $^{34\text{-}36}$ therefore a single magnetic momentum vector $\vec{\mu}$ along the axis of easy magnetization (easy axis), a crystalline direction energetically favorable for the magnetization. This magnetic state is known as superparamagnetism 34,35 since the total magnetization is the sum the magnetic momentum of all atoms in the nanoparticle. At room temperature, the nanoparticle's magnetic momentum can fluctuate between the two equivalent directions along the easy axis, since the thermal energy is sufficient to overcome the anisotropy energy barrier, $E_B = KV$, in the absence of magnetic field, where K is the uniaxial magnetic anisotropy constant and V the NP volume.

The colloidal solution, in the absence of external magnetic field, does not present a resultant magnetization since there is a random orientation of the nanoparticles easy axis, and is optically isotropic. The magnetic moment of each nanoparticle tends to align to uniform external magnetic fields by two main mechanisms, 37,38 the Néel mechanism, in which the magnetic moment is deviated from the easy axis, or the Brownian mechanism, in which the crystalline structure physically rotates as a whole. The latter is the main mechanism of alignment when ferrofluids are subjected to external fields and it's characteristic time is of the order of hundreds of μ s.

Besides the alignment of individual magnetic moments parallel to the external field, the dipole-dipole interaction between nanoparticles in solution can induce the formation of aggregates⁴⁰ according to the magnitude of the applied field. It is known the existence of different regimen of aggregation, with two critical fields, H_{C1} and H_{C2} .²¹ If the magnitude of applied magnetic field H is that $H < H_{C1}$, a preferential direction is induced and the magnetic moments tends to align to the external field but no spatial structure is present since thermal energy prevents the aggregation of nanoparticles. For $H_{C1} < H < H_{C2}$, NP's are aggregated in a chain-like structure, which aspect-ratio increases progressively with the increase of the external field. On the other hand, if $H > H_{C2}$ there's a lateral aggregation of nanochains, forming bundles.^{16,21} In this case, the light scattering by the formed structures is significantly higher than the other cases.²¹ Espinosa and co-workers³⁰ have shown, for a system composed by magnetite nanoparticles under the effect of an external magnetic field of magnitude H = 1000 G, that chain-like structures of about one nanoparticle wide and five NP's long are formed.

2.2 Hyper-Rayleigh scattering

Hyper-Rayleigh scattering (HRS)^{32,33,41–43} corresponds to the incoherent elastic scattering of frequency-doubled radiation with respect the pump beam, as observed by Terhune and coworkers in 1965,⁴⁴ and it is commonly used to measure the first-order hyperpolarizability of molecules and particles in solution without the need to use external electric fields in order to create a preferential direction.

As described by Buckingham and coworkers, 45,46 an atom or molecule when subjected to a strong electric field \vec{E} presents an induced dipole momentum $\vec{\mu}$ in the (tensorial) form:

$$\mu_i = \alpha_{ij}E_i + \beta_{ijk}E_iE_k + \gamma_{ijkl}E_iE_kE_l + \dots \tag{1}$$

where α_{ij} is the linear polarizability and β_{ijk} and γ_{ijkl} are the first- and second-order hyperpolarizabilities, respectively, with numerical factors already incorporated in the tensors.⁴² The first-order hyperpolarizability β is zero for systems that present inversion symmetry since is an even-order nonlinearity.^{27,46}

Nevertheless, on liquids and colloidal solutions, fluctuations of molecular orientation are the main source of local symmetry breaking, ⁴² enabling the observation of even-order nonlinear processes. Thus, the scattered intensity $I(2\omega)$ in the hyper-Rayleigh experiment corresponds to the contribution of molecules on the solution, proportionally to the orientational average over the squared hyperpolarizability tensor, ^{47,48} $\langle \beta_{\text{HRS}}^2 \rangle$, in the form:

$$I(2\omega) = GN\langle \beta_{HRS}^2 \rangle I^2(\omega), \tag{2}$$

where $I(\omega)$ is the fundamental beam intensity, N is the concentration of scattering units and G an experimental parameter related to geometrical factors as well as instrumental quantities.

To determine the hyperpolarizability the external reference method⁴⁹ (ERM) is usually used, in which the scattering amplitude of a standard material (ref) is measured in addition to the sample without the modification of the experimental parameter G, changing the concentration of scattering units N for both the sample and the reference. The quadratic coefficients $I(2\omega)/I^2(\omega)$ is linearly dependent of N and the proportionality constant is $a_{ref} = G\beta_{ref}^2$ and $a_{sample} = G\beta_{sample}^2$ for the external reference and the sample, respectively. Since the hyperpolarizability of the reference β_{ref} is known, the sample's hyperpolarizability is given by:

$$\beta_{sample} = \beta_{ref} \sqrt{\frac{a_{sample}}{a_{ref}}}. (3)$$

Considering (X, Y, Z) the laboratory coordinate system of reference, the experiment was setup so the incident beam propagates along the X axis and the scattered signal along the Y direction. For the case where the incident beam is polarized along the Z direction, considering that the detection is not sensible to the polarization state of light, the measured hyperpolarizability is given by:^{48,50}

$$\beta = \sqrt{\langle \beta_{\text{HRS}}^2 \rangle} = \sqrt{\langle \beta_{\text{XZZ}}^2 \rangle + \langle \beta_{\text{ZZZ}}^2 \rangle},\tag{4}$$

where $\langle \beta_{\rm XZZ}^2 \rangle$ and $\langle \beta_{\rm ZZZ}^2 \rangle$ corresponds to tensorial macroscopic averages while the first subscript is related to the polarization state of the scattered light. Despite the fact that the macroscopic average $\langle \beta_{\rm HRS}^2 \rangle$ can be written as a function of molecular hyperpolarizability tensor components, $^{48,50-52}$ the determination of the tensorial components of the nanoparticles are beyond the scope of this work.

3. EXPERIMENTAL

For this work we studied magnetite (Fe₃O₄) nanoparticles in colloidal suspension that are commercially available (fluidMAG-OS from ChemicellTM), coated with oleic acid molecules in order to prevent aggregation and dispersed on double-distilled water, ddH₂O. Physical properties of the nanoparticles, as the mean diameter of crystalline magnetite cores and the size-distribution function, were determined previously, ²⁸ by x-rays diffraction (XRD) and transmission electron microscopy (TEM). From XRD measurements it was determined that $D_{\text{XRD}} = 16(1)$ nm, while from TEM, a large number of nanoparticles was studied and a lognormal distribution fitted to histogram of diameters, resulting in the median $D_{\text{TEM}} = 10.7$ nm and the standard deviation $\sigma_{\text{TEM}} = 0.3$ nm. Since the relation $\sigma_{\text{TEM}} = 0.3$ magnetic results are compatible.

To properly understand experimental results they must be normalized by the concentration of the basic units involved on the interaction with light. In magnetite, the light absorption for the visible and near infra-red range involves electronic transitions from the iron atoms located in the tetrahedral and octahedral sites^{28,54,55} of the spinel crystalline structure. Since the material's energy-level structure is related to the magnetite unit itself, Fe_3O_4 , it corresponds to the basic unit of interaction with light in our system²⁹ instead of individual atoms. The number of nanoparticles in the solution also isn't the proper normalization unit since systems composed of particles with different diameters would present different absorption coefficients even if the total amount

of NPs were the same. Therefore, for magnetite colloids with known volume fraction of solid material ϕ , the concentration N of basic units can be calculated as:

$$N = \frac{\rho N_A}{M} \phi,\tag{5}$$

where ρ is the magnetite mass density (5.18 g/cm³), N_A the Avogadro's number and M the magnetite molar mass (231.6 g/mol). This method allows the comparison with measurements made on other systems, such as solutions with nanoparticles of different sizes or shapes.

The measurement of attenuation spectrum was performed on samples with concentration in the range from 4.3×10^{16} to 2.0×10^{17} units of Fe₃O₄ per cubic centimeter, for wavelengths from 350 nm to 900 nm with a Shimadzu UV-1800 spectrometer, with the samples filling a 1 mm thick glass cuvette. In order to acquire the spectrum also in the presence of external magnetic field additional measurements were performed from 350 nm to 1100 nm using an Ocean Optics USB4000 spectrometer and the light source DH-2000-BAL, Mikropack, containing deuterium and tungsten halogen lamps. In this case, all samples were conditioned in 10 mm quartz cuvettes. The magnetic field was applied with permanent circular neodymium magnets of 12 cm of diameter, positioned so the field's magnitude was H = 800 G.

Hyper-Rayleigh scattering measurements were performed with diluted samples, with concentration of magnetite units, N[Fe₃O₄], between 1.4×10^{16} and 5.3×10^{16} units/cm³, condition found to present intense nonlinear signal and low light attenuation, using and extension⁵⁶ of the conventional setup. For this purpose was used an infra-red beam (1064 nm), emitted by a solid state Nd:YAG (Coherent Inc., Antares 76-S) laser, modulated both by a mode-locker and a Q-switcher. Mode-locked pulses had the duration of 100 ps (FWHM), separated by 13 ns and, due to the Q-switch envelope (150 ns FWHM), their intensity was different from each other, allowing measurements as a function of the incident intensity (satisfying Eq. 2) without requiring additional optical elements.⁵⁶

The the beam was focalized in the center of a 10 mm cuvette, in which the solution was placed, and the nonlinear scattered signal was detected by a photo-multiplier tube (PMT), perpendicularly to the incident beam, as illustrated on Fig. 1. To avoid light from other sources, the sample and the PMT were placed inside a black box of dimensions $50 \text{ cm} \times 30 \text{ cm} \times 30 \text{ cm}$. At the entrance of the black box a narrow band-pass filter centered at 1064 nm (F₁₀₆₄) was placed and another band-pass filter, centered at 532 nm, was placed in the front of the PMT, assuring the detection of the scattered light only. With the purpose of increasing the signal-to-noise ratio, a spherical mirror was placed at the opposite direction of the PMT. The intensity of the incident beam, acquired by a fast silicon detector (Ref), and the scattered signal were registered by an oscilloscope and a microcomputer, that controlled an electric-mechanical shutter in order to block sample illumination for long periods.

For the development of Eq. 2 there is the hypotheses that neither the fundamental beam nor the second harmonic light is attenuated within the sample. On magnetic colloids, the UV-Vis light attenuation or extinction is due to two processes occurring simultaneously:^{29,54,55} the linear absorption, due to electronic transitions between energy levels, and the Rayleigh scattering, that increases intensity following a $I_S \propto \lambda^{-4}$ law.

Thus, in the case where the second-harmonic is attenuated, but not the fundamental beam, the detected signal $S(2\omega)$ must be corrected to obtain the scattered intensity $I(2\omega)$ in order to maintain the validity of Eq. 2. For that, let $I^T(2\omega)$ be the total intensity of second harmonic generated at the center of the cuvette and scattered isotropically.⁵⁷ Therefore, $I(2\omega)$ corresponds to the the fraction of $I^T(2\omega)$ in the solid angle of detection. The $I(2\omega)$ to $I^T(2\omega)$ ratio taken into account by the G factor and the external reference method. Since the nonlinear signal is generated on the cuvette's center, part of the detected radiation, $i^D(2\omega)$, is collected directly by the lens and then collimated to the photo-multiplier tube, traveling half of the cuvette length within the sample. On the other hand, a fraction of the signal $(i^M(2\omega))$ is reflected by the spherical mirror through the sample before being detected, as presented on Fig. 1, thus travel-ling half of the cuvette length before reflection and the total length after it within the solution. Thereby, the intensity $S(2\omega)$ detected by the PMT is $S(2\omega) = i^D(2\omega) \times 10^{-\frac{1}{2} \text{Ext}(2\omega)} + i^M(2\omega) \times 10^{-\frac{3}{2} \text{Ext}(2\omega)}$, where $\text{Ext}(2\omega)$ is the optical density at the 2ω frequency for the total cuvette length. Since the focal distance of the lens and the radius of the spherical mirror are properly set, $i^D(2\omega) = i^M(2\omega) = \frac{1}{2}I(2\omega)$, as shown of figure 1. Thus $S(2\omega) = \frac{1}{2}I(2\omega) \left(10^{-\frac{1}{2} \text{Ext}(2\omega)} + 10^{-\frac{3}{2} \text{Ext}(2\omega)}\right)$, and

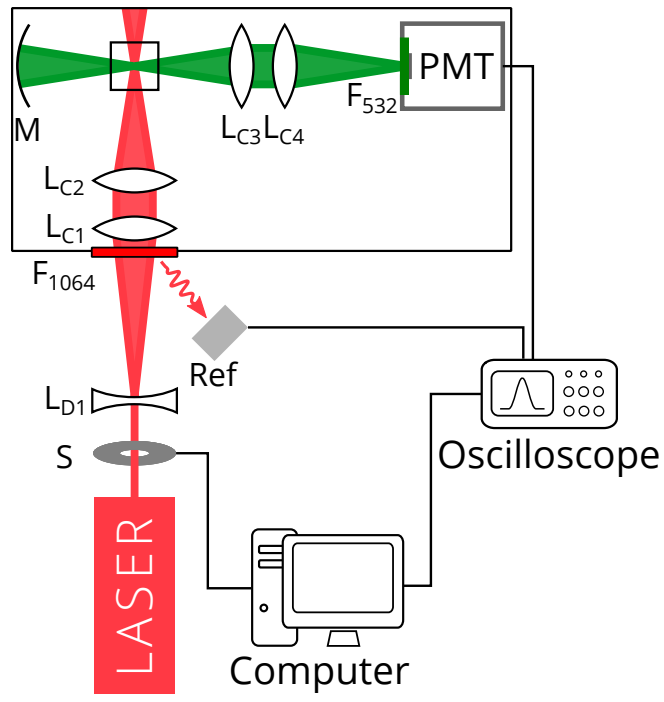


Figure 1. Diagram of HRS setup, composed by a mode-locked and Q-switched Nd:YAG laser emitting a light beam centered at $\lambda = 1064$ nm, that is focused on the center of a 10 mm cuvette after passing a narrow band-pass filter centered at 1064 nm (F₁₀₆₄) at the entrance of a black box. The incident intensity was detected by a fast silicon detector (Ref) and the nonlinear scattering detected at perpendicular direction by a photo-multiplier tube (PMT), after a 532 nm band-pass filter (F₅₃₂). A spherical mirror (M) at the opposite direction was used to increase the signal-to-noise ratio. An electric-mechanical shutter (S), controlled by a computer, was used in order to block sample illumination for long periods.

the total intensity of the scattered signal, corrected by the losses, is given by:

$$I(2\omega) = \frac{2S(2\omega)}{10^{-\frac{1}{2}\operatorname{Ext}(2\omega)} + 10^{-\frac{3}{2}\operatorname{Ext}(2\omega)}}.$$
(6)

The external reference method was used to determine quantitatively the hyperpolarizability of our samples, as described on equation 3. For that, the reference used was the p-nitroaniline (pNA) dissolved in DMSO (dimethyl sulfoxide), since it's first hyperpolarizability is well known in the literature, ⁵⁸ with concentrations between 1.7×10^{19} and 7.2×10^{19} molecules/cm³.

Measurements of nonlinear scattering amplitude of nanoparticles were also performed in the presence of external magnetic field of magnitude H=800 G, applied with circular neodymium magnets, 4.5 cm far from the focal region inside the sample. In this case, experiments were performed with the light polarization parallel to the magnetic field, parallel configuration, (H_{\parallel}) and perpendicular to the field, perpendicular case (H_{\perp}) .

4. RESULTS AND DISCUSSION

To comprehend the HRS results adequately, the light attenuation of wavelength that corresponds to the second harmonic, 532 nm, must be determined for all samples, and the detected signal corrected according to equation 6. Thus, as shown in the attenuation spectrum presented on Fig. 2(a) for wavelengths from 350 nm to 900 nm, our samples exhibits minimal extinction of light around 700 nm and doesn't change within the experimental errors for higher wavelengths in the range of concentrations studied. For smaller wavelength the attenuation increases due to both the linear Rayleigh scattering and to linear absorption. The optical density as a function of the concentration of magnetite units is shown on Figure 2(b) for the wavelength $\lambda = 532$ nm, displaying a linear

dependency as expected by the Beer-Lambert model, validating the choice of magnetite unit as the basic unit of interaction with light. Experimental points were fitted with a linear function (solid line) that was, then, used to calculate the light attenuation by all samples studied by the HRS technique. This method was preferred rather than direct measurements of lower concentrated samples because the extinction coefficient for those samples is near the limit of the spectrometer's resolution, leading to high relative errors that would propagate to HRS results.

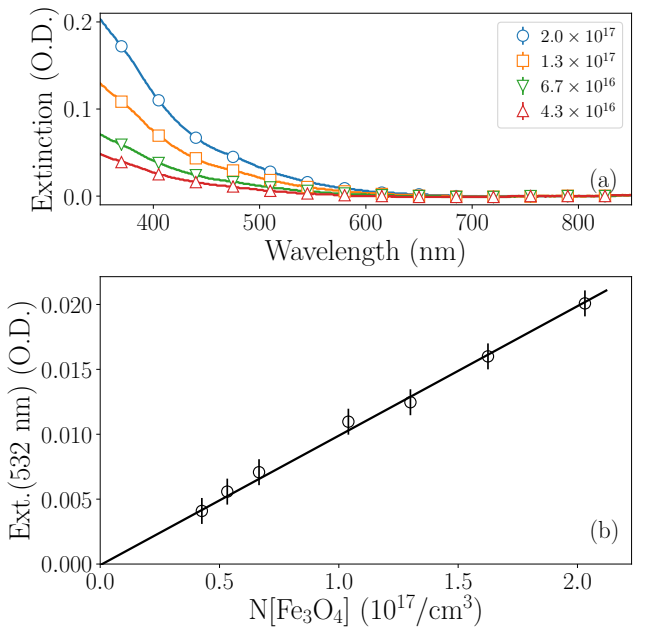


Figure 2. (a) Light attenuation spectra of ferrofluids in different concentrations of magnetite units. In this case, the error bars are smaller than the point size presented (± 0.001). (b) Linear dependency of the optical density at 532 nm as with the concentration of magnetite units. Figure adapted from ³¹

In previous works where optical properties of ferrofluids were studied, ^{29,59} the possibility of spurious effects due to cumulative phenomena was verified. Thus, in order to ensure the nonexistence of physical effects aside from the nonlinear scattering, HRS measurements were performed for the most concentrated sample as a function of the Q-switcher repetition rate, between 5 Hz and 800 Hz, without changes on the mode-locker. The amplitude of the scattered signal should not change with the repetition rate if cumulative effects were not present on the system. Thus, the scattered signal corrected by the attenuation $I(2\omega)$ is shown as a function of the incident intensity $I(\omega)$ for the Q-switcher repetition rate of 5 Hz, 10 Hz, 30 Hz, 50 Hz, 100 Hz, 300 Hz, 500 Hz and 800 Hz at Fig. 3, where the points corresponds to experimental data and the lines to visual guidance. Results obtained for rates smaller than and equal to 50 Hz are compatible to each other since the curves overlap, indicating that cumulative effects are not present during these measurements, since changing the time between two consecutive pulse trains didn't modify the results. Results obtained at 100 Hz are systematically smaller than the ones for smaller repetition rates for $I(\omega)$ between 0.10 and 0.20 and increases faster for $I(\omega) > 0.20$, indicating that the expected quadratic relationship between the scattered signal and the incident beam is not satisfied. This is more evident for higher rates, where the detected signal decreases as the repetition rate increases, meaning that there isn't enough time for the sample to relax between two pulse trains, leading to cumulative effects in our samples for measurements performed with rates equal to and higher than 100 Hz.

Further studies of the Q-switcher repetition rate can be seen on Fig. 4, where the scattered intensity is plotted as a function of the incident intensity in log scale for 30 Hz and 300 Hz. In order to verify the validity of Eq. 2, a power law was fitted to the experimental results in order to determine the best exponent to the relation $I(2\omega) \propto I(\omega)^n$. Measurements performed at 30 Hz present a quadratic relationship, with n = 2.1(1) as the optimum exponent. On the other hand, for measurements at 300 Hz the power law that best describe the

data has n = 2.6(1) as the exponent, confirming the previous hypotheses that in this case additional phenomena are present during the experiments, besides the nonlinear scattering.

After studying the nonlinear signal as a function of Q-switcher repetition rate, the nonlinear scattering amplitude was studied as a function of the number of magnetite units at the rate of 30 Hz, ensuring the nonexistence of spurious effects during the measurements. The exponential analysis presented on Fig. 4 was performed for all concentrations and, for every case, the optimum fitted parameter n was compatible to the expected value (n=2). Therefore, the following HRS analysis was performed by fitting a quadratic function to the data, with the quadratic coefficient as the fitting parameter, rather than the exponential method since the theoretical framework is well established and all the exponents are compatible to the expected value.

Thus, on Fig. 5(a) is shown typical curves of the nonlinear scattered intensity $I(2\omega)$ as a function of the fundamental beam irradiance $I(\omega)$ for some studied concentrations. Each experimental point corresponds to the average of 5000 data and the error bars are the corresponding standard deviation. The results were fitted by a quadratic function and the fitting parameter, the quadratic coefficient $I(2\omega)/I^2(\omega)$ is show on Fig. 5(b) as a function of the concentration of magnetite units for all studied samples. The linear dependency verified on Fig. 5(b) is expected for systems presenting only nonlinear scattering, supporting the decision of working with low repetition rates. Therefore, the first hyperpolarizability of our magnetite nanoparticles was obtained through the external reference method by the analysis process described on Eq. 3. On our case, the reference was the para-nitroaniline (pNA) molecule dissolved in DMSO, with $\beta_{\rm pNA}=28.8\times10^{-30}~{\rm cm}^5/{\rm esu}$. The first-order hyperpolarizability of magnetite units calculated as $\beta=8.5(1)\times10^{-28}~{\rm cm}^5/{\rm esu}$, which has a similar order of magnitude when compared with the results found for other nanoparticles, such as metallic nanospheres of similar diameter, $^{60-62}$ normalized by the number of atoms.

After establishing a reliable way to measure the first-order hyperpolarizability of magnetite nanoparticles in colloidal solution, the effects of aligning the NP's through external magnetic field were investigated. The experiments were performed both in the parallel configuration (H_{\parallel}) , in which the light polarization and the field lines were in the same direction, and in the perpendicular case (H_{\perp}) , where the polarization and the field lines were in orthogonal directions. For that, a half-wave plate was used to change the polarization direction and, in order to keep the parameter G unchanged, was present during the entire experiment. For each configuration, measurements were carried out with the sample in the presence and in the absence of magnetic field, alternately, in order to guarantee that in both cases the sample concentration was the same, avoiding possible error sources during the determination of the hyperpolarizability.

In the absence of magnetic field the hyperpolarizability of our magnetic nanoparticles was determined by the external reference method, with pNA molecules as external reference and the incident polarization in the vertical

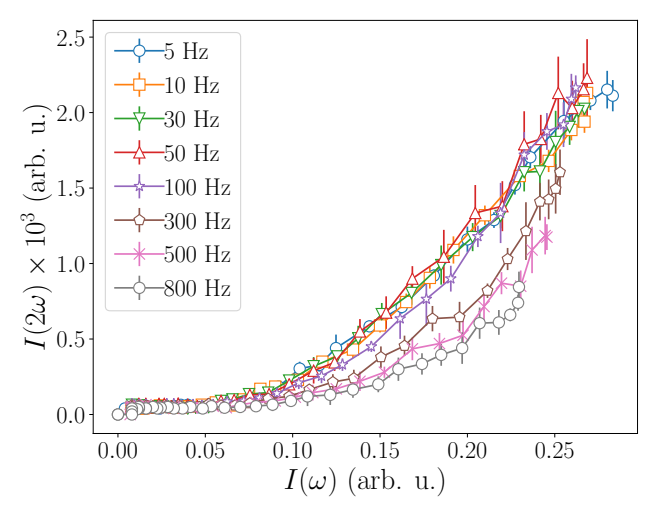


Figure 3. Nonlinear scattered signal $I(2\omega)$ as a function of the fundamental beam irradiance $I(\omega)$ for the most concentrated sample (N = 5.3×10^{16} units/cm³) measured at different Q-switcher repetition rates.

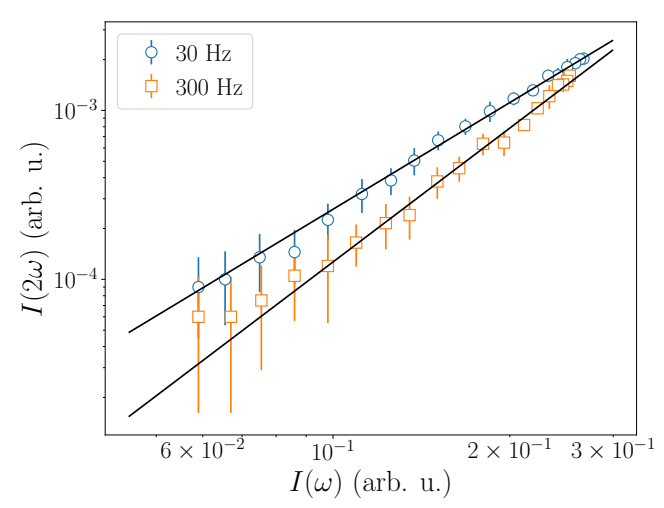


Figure 4. Logarithmic plot of nonlinear scattered signal $I(2\omega)$ as a function of the fundamental beam irradiance $I(\omega)$ for the most concentrated sample (N = 5.3×10^{16} units/cm³) measured at the Q-switcher repetition rates of 30 Hz and 300 Hz. For the former, the fitting of a power law resulted on the exponent n = 2.1(1), according to the model, while the latter n = 2.6(1).

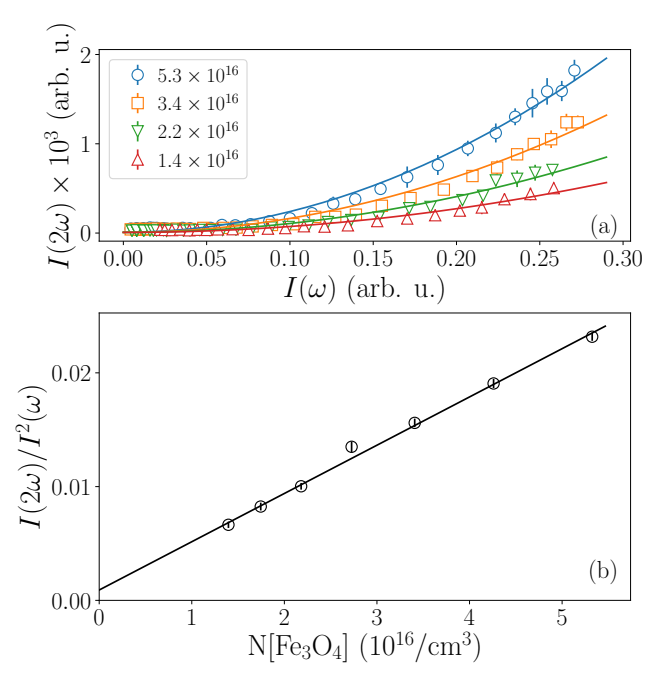


Figure 5. (a) Typical curves of nonlinear scattered signal $I(2\omega)$ as a function of the fundamental beam irradiance $I(\omega)$ and the correspondent quadratic fits. (b) Quadratic coefficient $I(2\omega)/I^2(\omega)$ as a function of the concentration of Fe₃O₄ units for studied all samples. The figure was adapted from 31

state. Since the β value was already determined for nonaligned nanoparticles it was then used as the external reference for the case that nanoparticles were subjected to the magnetic field, with the incident beam in the same polarization state.

Measurements of the scattering amplitude performed in the parallel configuration (H_{\parallel}) are presented on Fig. 6(a), where can be verified that the signal is increased when the external magnetic field is applied. In this case, the hyperpolarizability was calculated as $\beta_{\parallel} = 9.8(2) \times 10^{-28}$ cm⁵/esu. On the other hand, on figure 6(b) is shown the results for measurements performed on the perpendicular case (H_{\perp}) . For every concentration, in the presence of magnetic field the scattered signal decreases with respect the case H = 0, systematically, and the

difference is clearer for higher concentrations. The hyperpolarizability in the perpendicular configuration was then calculated as $\beta_{\perp} = 8.1(1) \times 10^{-28} \text{ cm}^5/\text{esu}$.

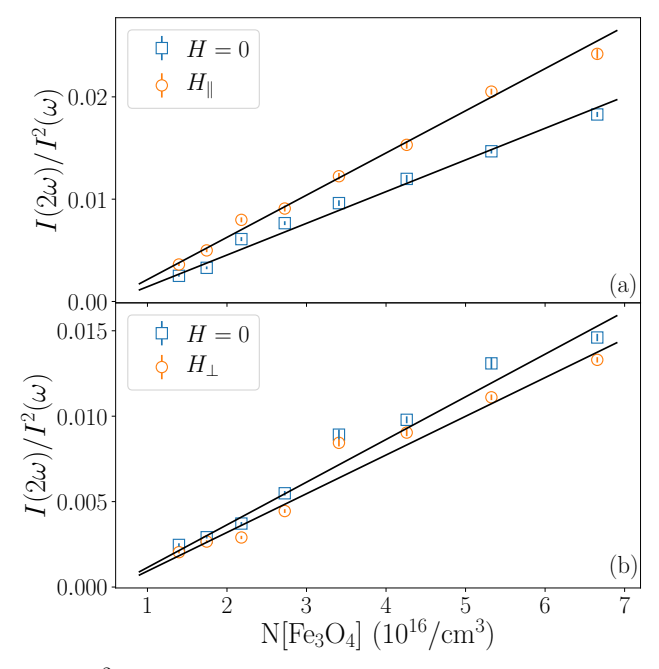


Figure 6. Quadratic coefficient $I(2\omega)/I^2(\omega)$ as a function of the concentration of Fe₃O₄ units in the absence (squares) and presence (circle) of the external magnetic field. The light polarization and magnetic field lines are: (a) in the same direction; (b) in orthogonal directions. Adapted from³¹

Small changes on the values of quadratic coefficients for the case H=0 can be verified when comparing results presented on figures 6(a) and 6(b), due to variations in the experimental factor G mainly due to fluctuations on laser power and small alignment changes. Nevertheless, these variations are taken into account by the external reference method, since the quadratic coefficient $I(2\omega)/I(\omega)^2 = G\beta^2N$ for each case can be numerically different, but the hyperpolarizability β for the nanoparticles in the absence of magnetic field is not.

The dynamics of magnetic nanoparticles in the presence of external magnetic fields is governed by two critical fields H_{C1} and H_{C2} , that controls the formation of small chains of nanoparticles or bigger aggregates. Since the measured attenuation spectrum does not change when the magnetic field is applied, its magnitude is smaller than the second critical field, $H < H_{C2}$, otherwise the linear scattering would increase drastically, modifying the light extinction spectrum. Therefore, for the magnitude of magnetic field applied, it's effect over the system consists on the alignment of each NP's magnetic momentum to the defined preferential direction. For systems composed by nanoparticles dispersed in liquid solution, it is known that the main mechanism of orientation is the Brownian rotation, where the crystalline structure of the nanoparticles rotates with respect the external field. Since the characteristic time of this phenomenon is of the order of hundreds of microseconds, $^{37-39}$ measurements of nonlinear optical properties take place after the nanoparticles are already aligned to the field's direction. Hence, the Brownian rotation only affects the obtained results by aligning the nanoparticles in the solution and, since the nanoparticles are mono-crystalline, the alignment of the magnetic momentum induces the alignment of specific crystallographic planes. Thereby, the differences in the measured hyperpolarizability values are a consequence of the anisotropy of the hyperpolarizability.

The direction of easy magnetization for magnetite corresponds to the $\langle 111 \rangle$ direction.^{34,63} Therefore, when the light polarization and the field are parallel, the measured hyperpolarizability β_{\parallel} corresponds to the hyperpolarizability along the $\langle 111 \rangle$ crystallographic direction while on the perpendicular case the hyperpolarizability β_{\perp} corresponds to the average of the other two equivalent directions perpendicular to the axis of easy magnetization, that is, letting the x-axis of the particle reference frame be parallel to the easy axis direction, $\beta_{\parallel} = \beta_{xxx}$, and β_{\perp} corresponds to a average from β_{yyy} and β_{zzz} . In the absence of magnetic field, however, there is no alignment

and $\beta_{H=0}$ corresponds to the average of all orientations. This can be verified calculating the average hyperpolarizability for the two cases in which the external field was applied, $\langle \beta_H \rangle = \frac{1}{3} \left(\beta_{\parallel} + 2\beta_{\perp} \right) = 8.6(1) \times 10^{-28} \text{ cm}^5/\text{esu}$, which corresponds to the average over the three orthogonal directions and is compatible with the value measured for the system without magnetic field $\beta_{H=0} = 8.5(1) \times 10^{-28} \text{ cm}^5/\text{esu}$. Therefore, the first-order optical hyperpolarizability of magnetite shows an anisotropy $\frac{\beta_{\parallel} - \beta_{\perp}}{\beta_{\parallel}}$ of about 17%.

5. CONCLUSIONS

In order to determine the first order hyperpolarizability of magnetite nanoparticles dispersed on aqueous solution the hyper-Rayleigh scattering technique was used. The experimental setup was composed by a mode-locked and Q-switched laser emitting pulse trains of 100 ps on an envelope of 150 ns and, seeking to determine the best experimental procedure to avoid spurious and cumulative effects during the measurements, the results were studied for different values of the Q-switcher repetition rate, from 5 Hz to 800 Hz. For rates smaller than 50 Hz the quadratic dependency between the nonlinear scattered signal amplitude and the incident intensity was verified within the experimental errors meaning that spurious effects were not present in our system, unlike measurements at higher repetition rates that changed as the rate was increased. Therefore, it was determined that all measurements would be performed at the rate of 30 Hz. Furthermore, effects of magnetic field were studied subjecting the samples to a uniform field of magnitude H = 800 G. Measurements were performed in the parallel configuration, where the incident beam polarization and magnetic field lines were oriented in the same direction, and in the perpendicular configuration, where the light polarization direction was orthogonal to the field lines. In the absence of external magnetic field, $\beta_{H=0}=8.5(1)\times 10^{-28}~{\rm cm}^5/{\rm esu}$, while for the parallel configuration $\beta_{\parallel}=9.8(2)\times 10^{-28}~{\rm cm}^5/{\rm esu}$ and in the perpendicular, $\beta_{\perp}=8.1(1)\times 10^{-28}~{\rm cm}^5/{\rm esu}$. As the crystalline structure of the nanoparticles rotates in order to align their magnetic moment to the external magnetic field, the differences are due to the hyperpolarizability anisotropy. Defining the x-axis of the particle reference frame parallel to the $\langle 111 \rangle$ crystallographic direction, which corresponds to the direction of easy magnetization, $\beta_{\parallel} = \beta_{xxx}$, and β_{\perp} corresponds to a average from β_{yyy} and β_{zzz} . In the absence of external field, the nanoparticles are randomly oriented and the measured hyperpolarizability corresponds to an average over the three orthogonal directions, $\langle \beta_H \rangle = \frac{1}{3} \left(\beta_{\parallel} + 2\beta_{\perp} \right) = 8.6(1) \times 10^{-28} \text{ cm}^5/\text{esu.}$

ACKNOWLEDGMENTS

The authors thanks the following funding agencies for their financial support: CNPq (Conselho Nacional de Desenvolvimento Científico e Tecnológico) (465259/2014-6; 404541/2016-0), FAPESP (Fundação de Amparo à Pesquisa do Estado de São Paulo) (2008/57685-7; 2011/13616-4; 2015/20555-2; 2016/20886-1), CAPES (Coordenação de Aperfeiçoamento de Pessoal de Nível Superior), INCT-FCx (Instituto Nacional de Ciência e Tecnologia de Fluidos Complexos), INCT-INFO (Instituto Nacional de Ciência e Tecnologia de Fotônica), NAP-FCx (Núcleo de Apoio à Pesquisa de Fluidos Complexos).

REFERENCES

- [1] C. Scherer and A. M. Figueiredo Neto, "Ferrofluids: properties and applications," *Brazilian Journal of Physics* **35**(3A), pp. 718–727, 2005.
- [2] A. M. Figueiredo Neto and S. R. A. Salinas, The physics of lyotropic liquid crystals: phase transitions and structural properties, Monographs on the physics and chemistry of materials, Oxford University Press, New York, 2005.
- [3] R. E. Rosensweig, Ferrohydrodynamics, Dover Publications, Inc, Mineola, New York, dover edition ed., 2014.
- [4] R. Banerjee, Y. Katsenovich, L. Lagos, M. McIintosh, X. Zhang, and C.-Z. Li, "Nanomedicine: magnetic nanoparticles and their biomedical applications," *Current medicinal chemistry* 17(27), pp. 3120–3141, 2010.
- [5] J. Durán, J. Arias, V. Gallardo, and A. Delgado, "Magnetic colloids as drug vehicles," *Journal of Pharmaceutical Sciences* **97**(8), pp. 2948–2983, 2008.
- [6] A. Ito, M. Shinkai, H. Honda, and T. Kobayashi, "Medical application of functionalized magnetic nanoparticles," *Journal of Bioscience and Bioengineering* **100**(1), pp. 1–11, 2005.

- [7] R. Hiergeist, W. Andrä, N. Buske, R. Hergt, I. Hilger, U. Richter, and W. Kaiser, "Application of magnetite ferrofluids for hyperthermia," *Journal of Magnetism and Magnetic Materials* **201**(1), pp. 420–422, 1999.
- [8] I. Torres-Díaz and C. Rinaldi, "Recent progress in ferrofluids research: novel applications of magnetically controllable and tunable fluids," *Soft Matter* **10**, pp. 8584–8602, Sept. 2014.
- [9] J. Philip and J. M. Laskar, "Optical Properties and Applications of Ferrofluids—A Review," Journal of Nanofluids 1, pp. 3–20, June 2012.
- [10] H. V. Thakur, S. M. Nalawade, S. Gupta, R. Kitture, and S. N. Kale, "Photonic crystal fiber injected with \$\text{Fe}_3 \text{O}_4\$ nanofluid for magnetic field detection," Applied Physics Letters 99, p. 161101, Oct. 2011.
- [11] A. Candiani, M. Konstantaki, W. Margulis, and S. Pissadakis, "Optofluidic magnetometer developed in a microstructured optical fiber," *Optics Letters* **37**, pp. 4467–4469, Nov. 2012.
- [12] Z. Zhang, T. Guo, X. Zhang, J. Xu, W. Xie, M. Nie, Q. Wu, B.-O. Guan, and J. Albert, "Plasmonic fiber-optic vector magnetometer," *Applied Physics Letters* **108**, p. 101105, Mar. 2016.
- [13] Y. Gu, G. Valentino, and E. Mongeau, "Ferrofluid-based reconfigurable optofluidic switches for integrated sensing and digital data storage," *Applied Optics* **53**, pp. 537–543, Feb. 2014.
- [14] A. El Amili, M. C. M. M. Souza, F. Vallini, N. C. Frateschi, and Y. Fainman, "Magnetically controllable silicon microring with ferrofluid cladding," *Optics Letters* **41**, pp. 5576–5579, Dec. 2016.
- [15] A. Duduś, R. Blue, and D. Uttamchandani, "Single-mode fiber variable optical attenuator based on a ferrofluid shutter," *Applied Optics* **54**, pp. 1952–1957, Mar. 2015.
- [16] J. M. Laskar, J. Philip, and B. Raj, "Experimental evidence for reversible zippering of chains in magnetic nanofluids under external magnetic fields," *Physical Review E* 80, Oct. 2009.
- [17] Y. Zou, Z. Di, and X. Chen, "Agglomeration response of nanoparticles in magnetic fluid via monitoring of light transmission," *Applied Optics* **50**, pp. 1087–1090, Mar. 2011.
- [18] W. H. Slade, E. Boss, and C. Russo, "Effects of particle aggregation and disaggregation on their inherent optical properties," Optics Express 19, pp. 7945–7959, Apr. 2011.
- [19] G. N. Rao, Y. D. Yao, Y. L. Chen, K. T. Wu, and J. W. Chen, "Particle size and magnetic field-induced optical properties of magnetic fluid nanoparticles," *Physical Review E* 72, Sept. 2005.
- [20] V. Socoliuc and L. Popescu, "Extinction of polarized light in ferrofluids with different magnetic particle concentrations," *Journal of Magnetism and Magnetic Materials* **324**, pp. 113–123, Jan. 2012.
- [21] S. Brojabasi, T. Muthukumaran, J. Laskar, and J. Philip, "The effect of suspended Fe3o4 nanoparticle size on magneto-optical properties of ferrofluids," *Optics Communications* **336**, pp. 278–285, Feb. 2015.
- [22] M. Saito and Y. Hirose, "Anisotropic transmission properties of magnetic fluids in the midinfrared region," Journal of the Optical Society of America B 28, pp. 1645–1649, July 2011.
- [23] R. Mehta, "Polarization dependent extinction coefficients of superparamagnetic colloids in transverse and longitudinal configurations of magnetic field," *Optical Materials* **35**, pp. 1436–1442, May 2013.
- [24] C. Rablau, P. Vaishnava, C. Sudakar, R. Tackett, G. Lawes, and R. Naik, "Magnetic-field-induced optical anisotropy in ferrofluids: A time-dependent light-scattering investigation," *Physical Review E* 78, Nov. 2008.
- [25] M. Adrian and L. E. Helseth, "Magnetically tunable optical absorbance in a colloidal system," Physical Review E 77, Feb. 2008.
- [26] Y. R. Shen, The principles of nonlinear optics, Wiley classics library, Wiley-Interscience, Hoboken, N.J., wiley classics library ed ed., 2003.
- [27] R. W. Boyd, Nonlinear Optics, Elsevier Science, Burlington, 1991.
- [28] D. Espinosa, L. B. Carlsson, A. M. Figueiredo Neto, and S. Alves, "Influence of nanoparticle size on the nonlinear optical properties of magnetite ferrofluids," *Physical Review E* 88(3), 2013.
- [29] D. Espinosa, E. S. Gonçalves, and A. M. Figueiredo Neto, "Two-photon absorption cross section of magnetite nanoparticles in magnetic colloids and thin films," *Journal of Applied Physics* **121**, p. 043103, Jan. 2017.
- [30] D. H. G. Espinosa, C. L. P. Oliveira, and A. M. Figueiredo Neto, "Influence of an external magnetic field in the two-photon absorption coefficient of magnetite nanoparticles in colloids and thin films," *Journal of the Optical Society of America B* **35**, pp. 346–355, Feb. 2018.

- [31] E. S. Gonçalves, R. D. Fonseca, L. De Boni, and A. M. Figueiredo Neto, "Tuning hyper-Rayleigh scattering amplitude on magnetic colloids by means of an external magnetic field," *Journal of the Optical Society of America B* **35**, p. 2681, Nov. 2018.
- [32] K. Clays and A. Persoons, "Hyper-Rayleigh scattering in solution," Physical Review Letters 66(23), pp. 2980–2983, 1991.
- [33] K. Clays and A. Persoons, "Hyper-Rayleigh scattering in solution," Review of Scientific Instruments 63, pp. 3285–3289, June 1992.
- [34] B. D. Cullity and C. D. Graham, *Introduction to Magnetic Materials*, John Wiley and Sons, New York, NY, 2011.
- [35] A. P. Guimarães, Principles of nanomagnetism, Nanoscience and technology, Springer, Heidelberg [Germany]; New York, 2009. OCLC: ocn416295448.
- [36] J. L. Dormann, D. Fiorani, and E. Tronc, "Magnetic Relaxation in Fine-Particle Systems," in Advances in Chemical Physics, I. Prigogine and S. A. Rice, eds., 98, pp. 283–494, John Wiley & Sons, Inc., Hoboken, NJ, USA, Jan. 1997.
- [37] R. Kötitz, P. C. Fannin, and L. Trahms, "Time domain study of Brownian and Néel relaxation in ferrofluids," Journal of magnetism and magnetic materials 149(1), pp. 42–46, 1995.
- [38] R. Rosensweig, "Heating magnetic fluid with alternating magnetic field," *Journal of Magnetism and Magnetic Materials* **252**, pp. 370–374, Nov. 2002.
- [39] R. Kötitz, W. Weitschies, L. Trahms, and W. Semmler, "Investigation of Brownian and Néel relaxation in magnetic fluids," *Journal of Magnetism and Magnetic Materials* **201**(1-3), pp. 102–104, 1999.
- [40] J. H. E. Promislow, A. P. Gast, and M. Fermigier, "Aggregation kinetics of paramagnetic colloidal particles," The Journal of Chemical Physics 102, pp. 5492–5498, Apr. 1995.
- [41] T. Verbiest, E. Hendrickx, A. P. Persoons, and K. J. Clays, "Measurements of molecular hyperpolarizabilities using hyper-Rayleigh scattering," 1775, pp. 206–212, Proc. SPIE, Feb. 1993.
- [42] K. Clays, Andre Persoons, and Maeyer, Leo, "Hyper-Rayleigh Scattering in Solution," in Modern Nonlinear Optics, Part 3, Myron Evans and Stanislaw Kielich, eds., Advances in Chemical Physics 85, pp. 455 – 498, Wiley, 1994.
- [43] K. Clays and A. Persoons, "Hyper-Rayleigh scattering in solution with tunable femtosecond continuous-wave laser source," *Review of Scientific Instruments* **65**, pp. 2190–2194, July 1994.
- [44] R. W. Terhune, P. D. Maker, and C. M. Savage, "Measurements of Nonlinear Light Scattering," Physical Review Letters 14(17), pp. 681–684, 1965.
- [45] A. D. Buckingham and J. A. Pople, "Theoretical Studies of the Kerr Effect I: Deviations from a Linear Polarization Law," *Proceedings of the Physical Society. Section A* **68**, pp. 905–909, Oct. 1955.
- [46] A. D. Buckingham and B. J. Orr, "Molecular hyperpolarisabilities," Quarterly Reviews, Chemical Society 21(2), p. 195, 1967.
- [47] G. J. T. Heesink, A. G. T. Ruiter, N. F. van Hulst, and B. Bölger, "Determination of hyperpolarizability tensor components by depolarized hyper Rayleigh scattering," *Physical Review Letters* 71, pp. 999–1002, Aug. 1993.
- [48] E. Hendrickx, K. Clays, and A. Persoons, "Hyper-Rayleigh Scattering in Isotropic Solution," Accounts of Chemical Research 31, pp. 675–683, Oct. 1998.
- [49] M. A. Pauley, H. Guan, C. H. Wang, and A. K. Jen, "Determination of first hyperpolarizability of nonlinear optical chromophores by second harmonic scattering using an external reference," *The Journal of Chemical Physics* 104, pp. 7821–7829, May 1996.
- [50] F. Castet, E. Bogdan, A. Plaquet, L. Ducasse, B. Champagne, and V. Rodriguez, "Reference molecules for nonlinear optics: A joint experimental and theoretical investigation," *The Journal of Chemical Physics* 136, p. 024506, Jan. 2012.
- [51] S. J. Cyvin, J. E. Rauch, and J. C. Decius, "Theory of Hyper-Raman Effects (Nonlinear Inelastic Light Scattering): Selection Rules and Depolarization Ratios for the Second-Order Polarizability," The Journal of Chemical Physics 43, pp. 4083–4095, Dec. 1965.
- [52] R. Bersohn, Y. Pao, and H. L. Frisch, "Double-Quantum Light Scattering by Molecules," *The Journal of Chemical Physics* **45**, pp. 3184–3198, Nov. 1966.

- [53] E. Tronc and D. Bonnin, "Magnetic coupling among spinel iron oxide microparticles by Mössbauer spectroscopy," *Journal de Physique Lettres* **46**(10), pp. 437–443, 1985.
- [54] W. F. J. Fontijn, P. J. Van der Zaag, M. A. C. Devillers, V. A. M. Brabers, and R. Metselaar, "Optical and magneto-optical polar Kerr spectra of $\text{C}_4\$ and $\text{C}_4\$ and $\text{C}_4\$ or $\text{C}_4\$ -3\text{Al}^{3+}\$ substituted $\text{C}_4\$ -3\text{O}_4\$," *Physical Review B* **56**(9), p. 5432, 1997.
- [55] W. F. J. Fontijn, P. J. van der Zaag, L. F. Feiner, R. Metselaar, and M. A. C. Devillers, "A consistent interpretation of the magneto-optical spectra of spinel type ferrites (invited)," *Journal of Applied Physics* 85(8), p. 5100, 1999.
- [56] P. L. Franzen, L. Misoguti, and S. C. Zilio, "Hyper-Rayleigh scattering with picosecond pulse trains," Applied Optics 47, pp. 1443–1446, Apr. 2008.
- [57] R. Dinkel, W. Peukert, and B. Braunschweig, "In situ spectroscopy of ligand exchange reactions at the surface of colloidal gold and silver nanoparticles," *Journal of Physics: Condensed Matter* 29, p. 133002, Apr. 2017.
- [58] J. N. Woodford, M. A. Pauley, and C. H. Wang, "Solvent Dependence of the First Molecular Hyperpolarizability of p-Nitroaniline Revisited," The Journal of Physical Chemistry A 101(11), pp. 1989–1992, 1997.
- [59] A. L. Sehnem, D. Espinosa, E. S. Gonçalves, and A. M. Figueiredo Neto, "Thermal Lens Phenomenon Studied by the Z-Scan Technique: Measurement of the Thermal Conductivity of Highly Absorbing Colloidal Solutions," *Brazilian Journal of Physics*, July 2016.
- [60] K. Das, A. Uppal, R. Saini, G. Varshney, P. Mondal, and P. Gupta, "Hyper-Rayleigh scattering from gold nanoparticles: Effect of size and shape," Spectrochimica Acta Part A: Molecular and Biomolecular Spectroscopy 128, pp. 398–402, July 2014.
- [61] B. Jain, A. K. Srivastava, A. Uppal, P. K. Gupta, and K. Das, "NIR Femtosecond Laser Induced Hyper-Rayleigh Scattering and Luminescence from Silver Nanoprisms," *Journal of Nanoscience and Nanotechnology* 10, pp. 5826–5830, Sept. 2010.
- [62] R. C. Johnson, J. Li, J. T. Hupp, and G. C. Schatz, "Hyper-Rayleigh scattering studies of silver, copper, and platinum nanoparticle suspensions," *Chemical Physics Letters* **356**, pp. 534–540, Apr. 2002.
- [63] L. R. Bickford, "Ferromagnetic Resonance Absorption in Magnetite Single Crystals," Physical Review 78, pp. 449–457, May 1950.